Heterogeneity-Projection Hard-Decision Color Interpolation Using Spectral-Spatial Correlation

Chi-Yi Tsai and Kai-Tai Song
Department of Electrical and Control Engineering, National Chiao Tung University
1001 Ta Hsueh Road, Hsinchu 300, Taiwan
E-mail: chiyi.ece91g@nctu.edu.tw; ktsong@mail.nctu.edu.tw

Appendix

B. Soft-Decision, Enhanced Soft-Decision and Hard-Decision Demosaicing Algorithms

To show the difference between the proposed hard-decision method and the existent soft-decision ones, we describe the key idea of these two types of decision-based demosaicing algorithms in this section. Fig. 12 presents the flowchart of each decision-based demosaicing algorithm. Fig. 12(a) shows the flowchart of the original soft-decision method, in which the former interpolation stage usually generates two interpolated images, one is horizontally interpolated and another one is vertically. The latter decision stage chooses a better one for each color pixel output. In other words, the output image of the original soft-decision method only contains horizontal and vertical interpolated color pixels without smooth ones. In the aforementioned section, we noticed that the optimal interpolation result needs to consider the horizontal, vertical and smooth interpolations together. Therefore, the demosaicing performance of the soft-decision method is limited because only two directional interpolations are under consideration.

To overcome this drawback, Omer *et al.* proposed the enhanced soft-decision dmosaicing algorithm that regards the soft-decision processing as a meta-algorithm to improve the performance of traditional interpolation methods in places they tend to fail. Fig. 12(b) illustrates the flowchart of enhanced soft-decision demosaicing algorithm, in which the former interpolation stage generates not only two directional interpolated images, but also a smooth interpolated one using a standard demosaicing method such as edge-directed schemes [17] or [20]. In the latter decision stage, two natural image properties, i.e. color variation and corner value, are employed as the demosaicing hints to evaluate a correct interpolation result and two erroneous ones. Although the enhanced soft-decision demosaicing algorithm provides more pleasing demosaiced results, the computation load in latter decision stage is increased greatly because it needs to evaluate three interpolation results.

Fig. 12(c) presents the flowchart of the proposed hard-decision demosaicing algorithm. Thanks to the proposed directional heterogeneity-projection and adaptive filtering schemes, the decision stage can be performed directly using the original Bayer mosaic image before interpolation stage. Moreover, the spatial classification also contains horizontal, vertical and smooth subsets for providing more accurate interpolation results in the latter stage. Therefore, the proposed hard-decision method provides comparable results using less computation than the enhanced soft-decision method does.

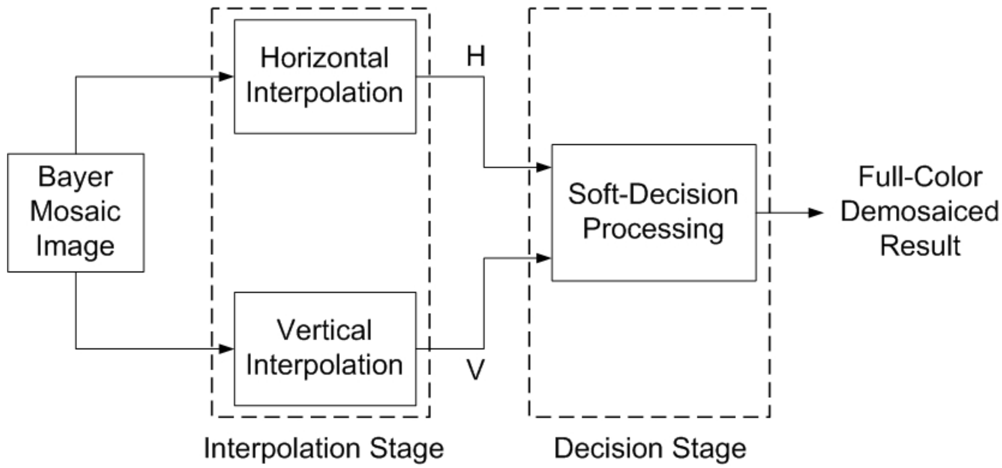

(a)

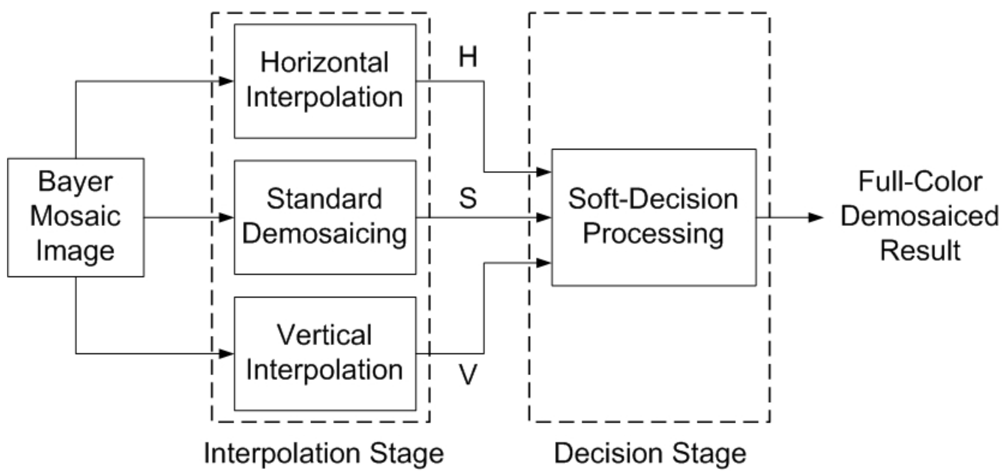

(b)

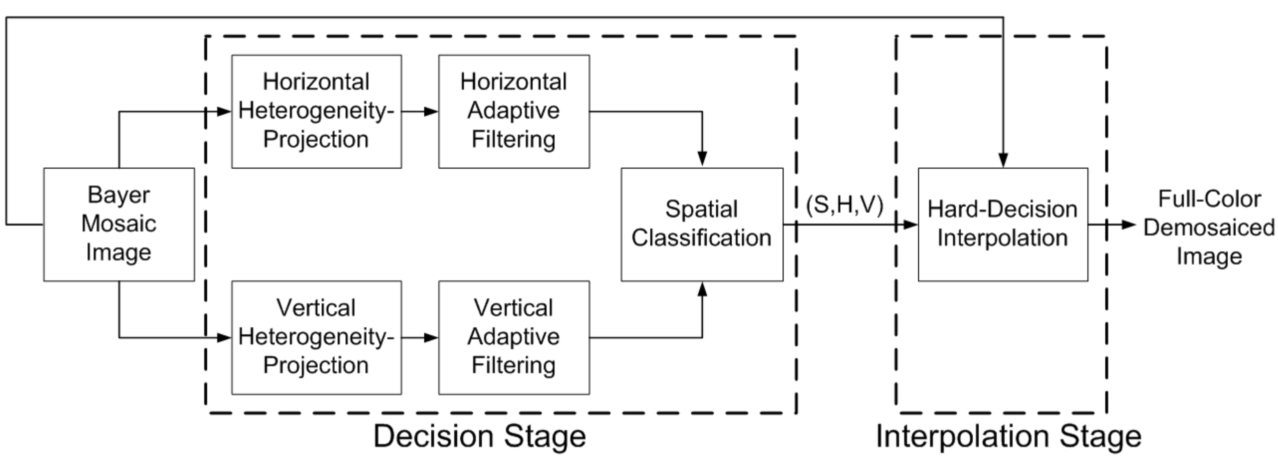

(c)

Fig. 12: Flowchart of the (a) soft-decision; (b) enhanced soft-decision and (c) proposed hard-decision algorithms.

C. Extended Visual Comparison

In this section, an extended study on visual comparison is presented using two images of 384×256 pixels taken from the Kodak database as shown in Fig. 13. We visually compared the performance of the proposed demosaicing method with six notable ones: Lu's [3], Gunturk's [5], Li's [6], Muresan's [4], Grossman's [9] and Omer's [10] methods. The parameter setting of [5] and [6] is the same as that in the manuscript. The results of [4] and [9] are obtained directly from the authors' web page in TIF and BMP formats, respectively. For Omer's method, the Kimmel's interpolation method [17] was employed to provide the smooth interpolated image in the interpolation stage.

For the proposed method, we first use the optimal parameters $(N_{opt}, \alpha_{opt}) = (11, 0.6)$ to reconstruct the Bayer mosaiced image of Lighthouse. The PSNR metric between the original and demosaiced images is 32.7315dB; however, there still are some noticeable color artifacts in the fence region. In order to reduce these noticeable color artifacts, we increase the values of (N, α) for estimating the horizontal and vertical edges accurately. After a tuning process, the suitable parameters are given by $(N, \alpha) = (24, 0.8)$ and the PSNR metric reduces to 32.4413dB. One can see that there is a tradeoff between quantitative and visual qualities. Fig. 14 shows the zoom-in of the demosaiced Lighthouse images using proposed method with parameters $(N_{opt}, \alpha_{opt}) = (11, 0.6)$ and $(N, \alpha) = (24, 0.8)$ respectively. Figs. 14(a) and (d) show the zoom-in of original Lighthouse in the fence and house regions, respectively. Figs. 14(b) and (e) show the corresponding zoom-in of demosaicing results using parameters $(N_{opt}, \alpha_{opt}) = (11, 0.6)$; Figs. 14 (c) and (f) show that using parameters $(N, \alpha) = (24, 0.8)$. Visually comparing these images, one can see that the demosaiced image using optimal parameters presents better result in house region than that using increased parameters, but some color artifacts still remain in fence region. On the

(a) (b)

Fig. 13: Test images used in the extended visual comparison. (a) Lighthouse. (b) Window.

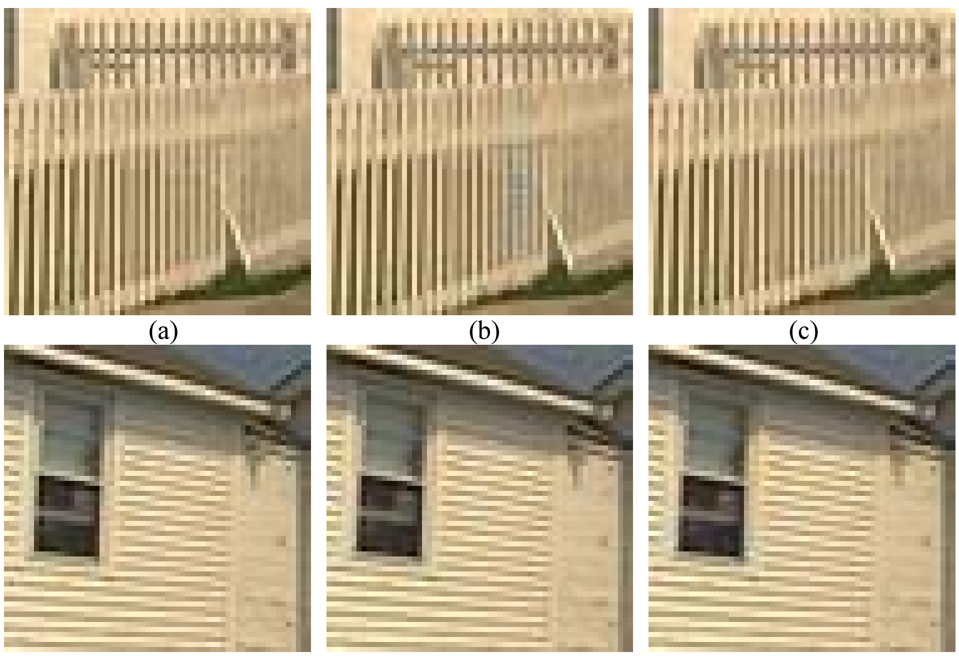

(a) (b) (c)

(d) (e) (f)

Fig. 14: (a) and (d) show the zoom-in of the original Lighthouse image in the fence and house regions, respectively. (b) and (e) show the zoom-in of the demosaicing results using parameters $(N_{opt}, \alpha_{opt}) = (11, 0.6)$. (c) and (f) show the zoom-in of the demosaicing results using parameters $(N, \alpha) = (24, 0.8)$.

contrary, the demosaiced image using increased parameters presents less color artifacts in fence region; however, the quality in house region is reduced. Therefore, the demosaicing results using increased parameters can reduce the color artifacts in the fence region but cannot provide better PSNR metric than those using optimal parameters.

For further visual comparison, we choose larger parameters $(N, \alpha) = (24, 0.8)$ for the proposed method, because it can provide more pleasing results in the fence region of the Lighthouse image. Figs. 15 and 16, respectively show the zoom-in of the Lighthouse demosaiced images in fence and house regions reconstructed by the methods under comparison. In Fig. 15, one can see that Muresan's, Grossman's and the HPHD-AI methods provide better demosaicing results in the fence region than the others do. However, in Fig. 16, one can see that the demosaicing result of Muresan's and Grossman's methods in house region induces more visible artifacts than the proposed method does. Therefore, the proposed method provides superior demosaicing result not only in fence region, but also in house region of the Lighthouse test image compared with other methods.

Fig. 17(a) shows the zoom-in of the original Window image in flower region, and Figs. 17(b)-(h) present the corresponding demosaiced results of the methods under comparison. Visually comparing these images shown in Fig. 17, one can see that the demosaicing images obtained by Lu's, Grossman's and the proposed method give more satisfactory results compared with others. Therefore, based on the above visual comparison, the performance improvement of the proposed HPHD-AI method on detail regions of the image is verified.

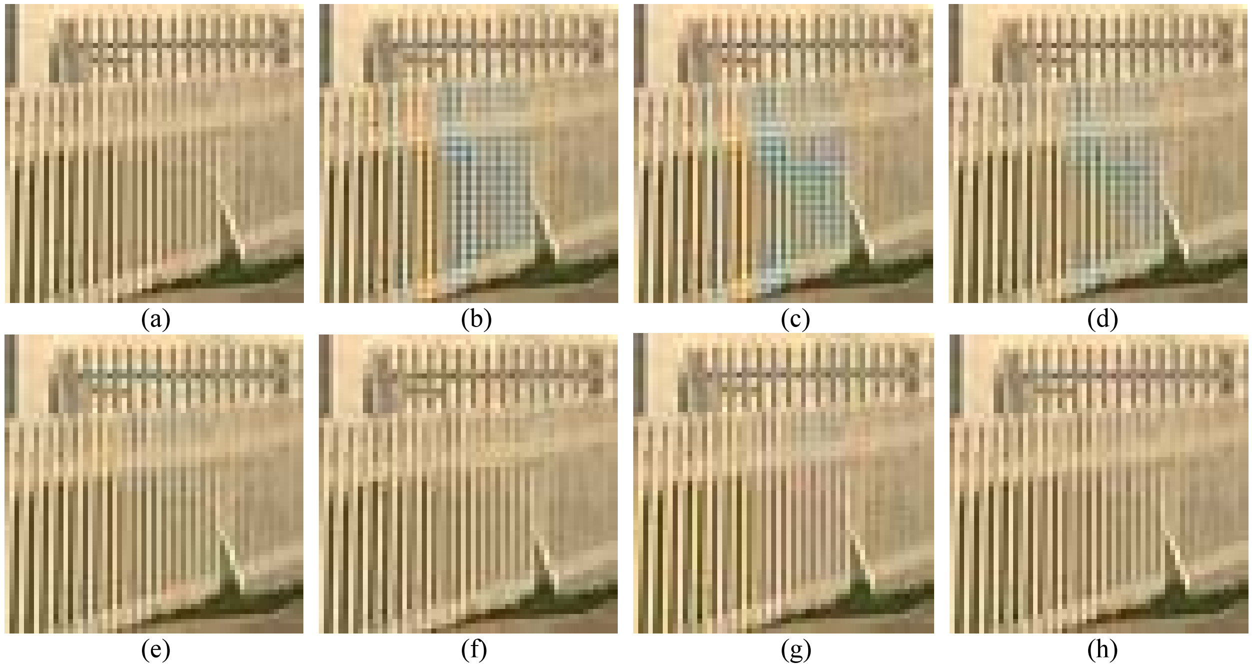

Fig. 15: Zoom-in demosaicing results of Lighthouse image in fence region. (a) Original picture; Demosaiced result in interpolation step: (b) Lu's method, (c) Gunturk's method, (d) Li's method, (e) Muresan's method, (f) Grossman's method, (g) Omer's method, (h) HPHD-AI method.

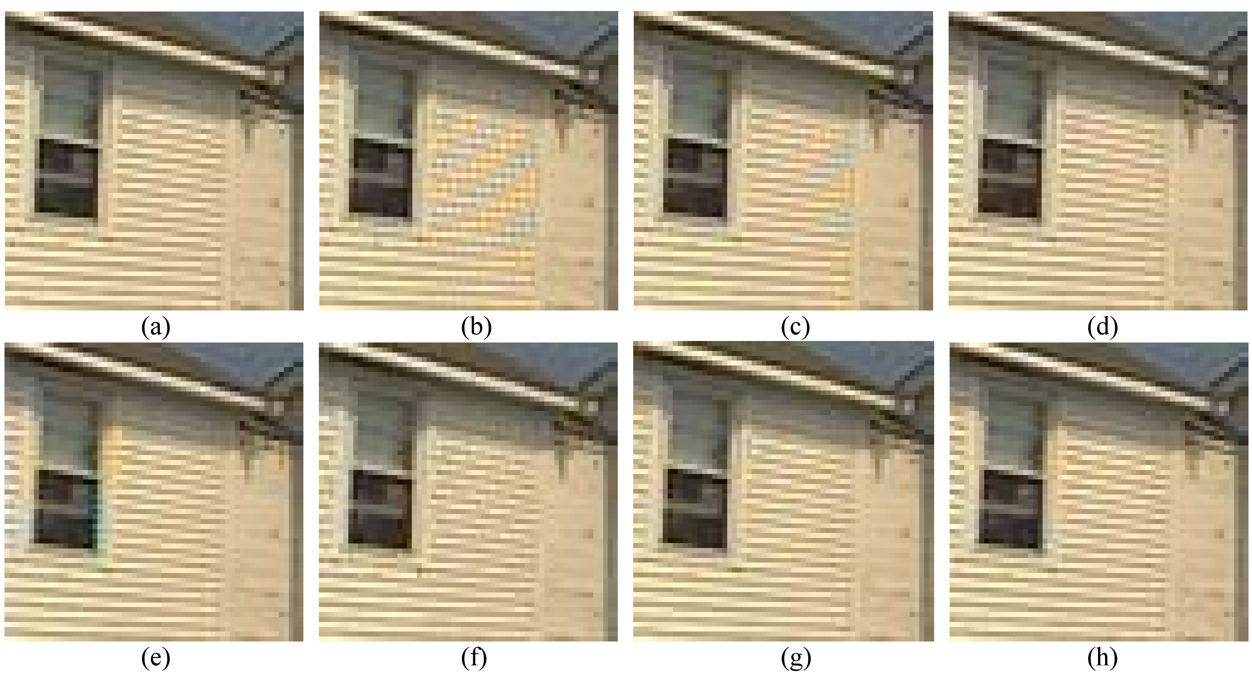

Fig. 16: Zoom-in demosaicing results of Lighthouse image in house region. (a) Original picture; Demosaiced result in interpolation step: (b) Lu's method, (c) Gunturk's method, (d) Li's method, (e) Muresan's method, (f) Grossman's method, (g) Omer's method, (h) HPHD-AI method.

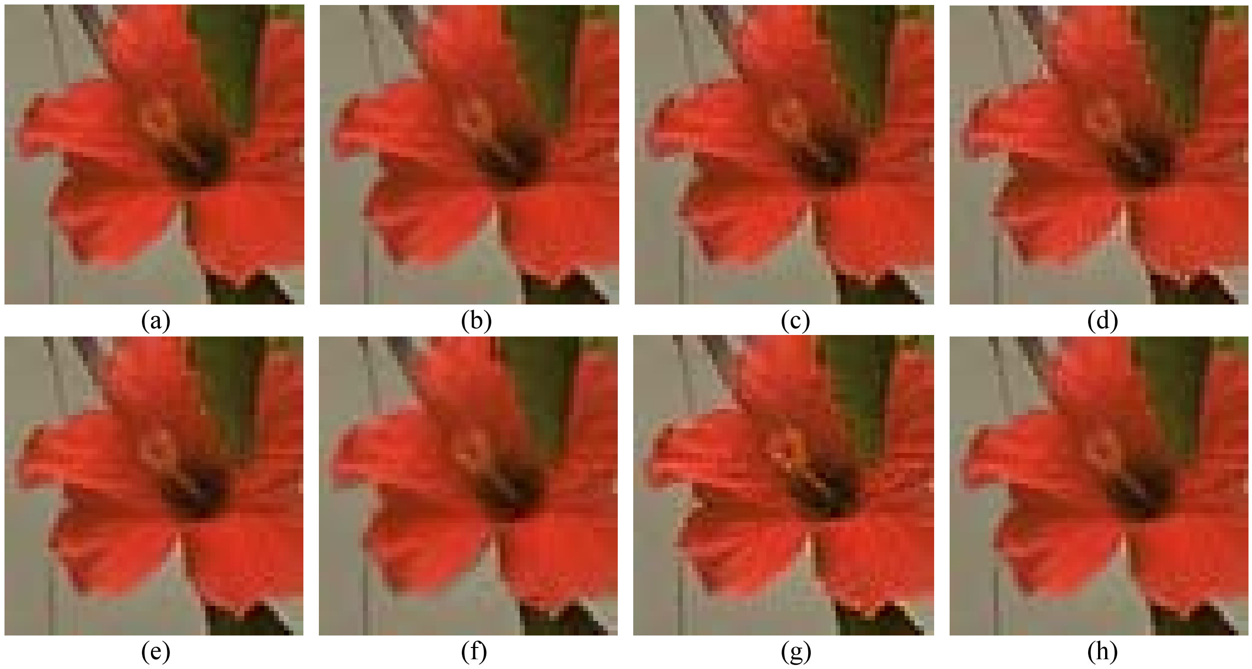

Fig. 17: Zoom-in demosaicing results of Window image. (a) Original picture; Demosaiced result in interpolation step: (b) Lu's method, (c) Gunturk's method, (d) Li's method, (e) Muresan's method, (f) Grossman's method, (g) Omer's method, (h) HPHD-AI method.